Solid Lipid–PEI Hybrid Nanocarrier: An Integrated Approach To Provide Extended, Targeted, and Safer siRNA Therapy of Prostate Cancer in an All-in-One Manner

Hui-Yi Xue[†] and Ho-Lun Wong[†,*]

[†]Department of Pharmaceutical Sciences, Temple University School of Pharmacy, 3307 North Broad Street, Philadelphia, Pennsylvania 19140, United States

ABSTRACT Small-interfering RNA (siRNA) has a high application potential for therapeutic silencing of pathologic or drug-resistance genes. However, although recent research has led to several nonviral nucleic acid delivery systems with encouraging transfection performance, there remains a substantial gap between these systems and an ideal siRNA carrier that can be safely and effectively used for the more complex delivery tasks such as cancer management. We hypothesized that by integrating the high transfection performance of linear polyethylenimine (PEI) with the controlled release properties of solid lipid components, and complementing the resulting lipid–PEI hybrid nanocarrier (LPN) with receptor-targeting capability, multiple limitations of the conventional siRNA carriers would be simultaneously overcome. Data comparing this new hybrid system with the conventional siRNA-PEI polyplexes showed 15 to 21% less loss of siRNA, higher selectivity for prostate cancer cells over noncancerous prostate cells, and significant reduction in both acute and delayed carrier toxicity especially to the noncancerous RWPE1 cells (*e.g.*, 71.2% of LPN-treated cells preserved proliferative capacity versus ≤30.2% in other groups). We further demonstrated sustained intracellular siRNA release from LPNs, which was shown translatable into extended *in vitro* and *in vivo* RNA-interference effects for a minimum of one week. Our findings generally support the use of LPN technology to achieve a longer-acting, less toxic, more efficient, and cancer-specific form of siRNA therapy in an "all-in-one" manner. This brings the nonviral siRNA delivery approach one important step closer to its clinical application.

KEYWORDS: small-interfering RNA · nonviral delivery · polyethylenimine · nanoparticle · cancer therapy

Small-interfering RNA (siRNA) provides the clinicians a highly promising tool to selectively turn off pathologic molecular pathways *via* the RNA-interference (RNAi) mechanism.[1,2] The prospect of applying siRNA for cancer therapy is especially appealing as it has been shown highly effective for silencing several oncogenic or chemoresistance pathways.[3,4] However, studies have also begun to identify its clinical limitations.[5–7] For instance, free siRNA molecules are known to have poor transfection efficiency and biological stability. Although these problems can be conveniently tackled using nonviral gene carriers, these carriers are often associated with significant normal tissue toxicity.[6–10] This toxicity issue is further complicated by the fact that the efficient carriers often cause unacceptable toxicity as a result of strong cell-carrier nonspecific interactions.[11–13] This poses a serious challenge to the development of safe and effective siRNA-based clinical treatment.

Polyethylenimine (PEI) is one of the most studied classes of polycationic polymers used as nonviral gene carriers. The high charge density of PEI molecules facilitates formation of well-condensed complexes with nucleic acids and interaction with cell surfaces,[14,15] and they are able to efficiently release nucleic acids from the endosomes by proton sponge effect.[16] The transfection efficiency of PEI is thus high among nonviral gene carriers. In addition, it is easily modifiable. Nevertheless, the aforementioned efficacy–toxicity correlation still applies to PEI.[11,12] To break this undesirable correlation, different strategies have been studied. These include the substitution of branched PEI with the less toxic, linear PEI,[17–19] development of easily degradable disulfide cross-linked PEI,[11] grafting branched PEI with hydrophobic moieties, and combining modified or unmodified PEI with liposomal ingredients to form "polycation liposomes" or similar submicrometer carriers.[16,20,21] Decreased toxicity and improved transfection efficacy was observed using these strategies for the delivery of DNA, and more recently, siRNA.

With this issue at least partly addressed, the next major challenge will be to equip the PEI-based systems for the more complex,

* Address correspondence to ho-lun.wong@temple.edu.

Received for review May 6, 2011 and accepted August 13, 2011.

Published online August 13, 2011
10.1021/nn201659z

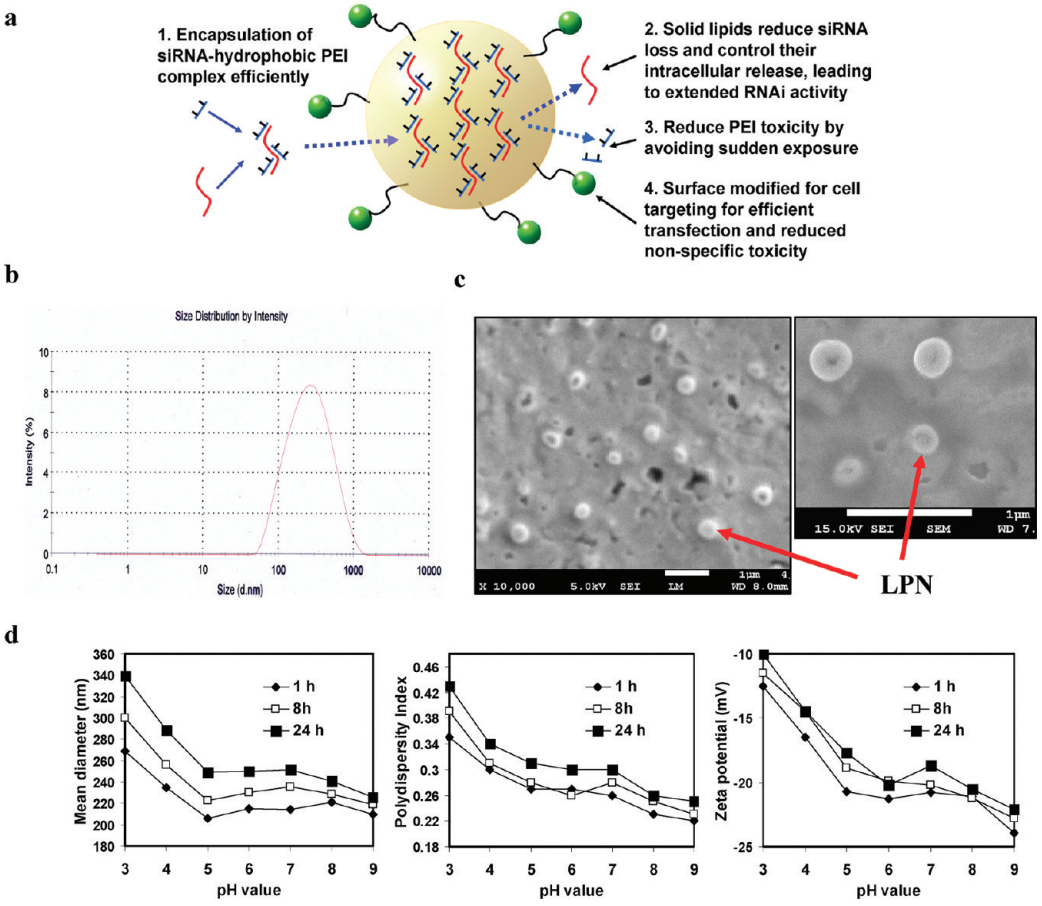

Figure 1. Design of a solid–lipid polyethylenimine hybrid nanoparticle (LPN), and its size, morphology, and pH response data. (a) Scheme illustrating the design of LPN and the hypotheses of using LPN to provide extended, targeted and safer siRNA therapy. siRNA molecules (red wavy curves) complexed with linear PEI molecules modified with hydrophobic groups (blue lines with short black branches) are physically encapsulated into nanocarrier core consisting mostly of solid lipids (pale yellow). The green surface groups represent targeting moieties (*e.g.* folate tagged phospholipids). (b) Size distribution of LPNs measured with photon correlation spectroscopy. Distribution by intensity is presented. (c) LPN images captured using scanning electron microscopy. Bar indicates 1 m. Left panel and right panel present images with low magnification (10,000×) and high magnification (25,000×), respectively. (d) pH responses of LPNs. Left panel: particle size; middle panel: polydispersity; right panel: zeta potential value. Mean values are presented.

demanding nucleic acid delivery tasks required for disease management, for instance, to develop high efficiency systems tailored for the delivery of the generally short-lived siRNA, with better control over the siRNA release kinetics and improved specificity for the target tissues. This will prove especially valuable for the management of cancers, which can greatly benefit from efficient, long-acting therapeutic action in the cancer cells and low carrier toxicity toward the non-cancer tissues at the same time.[22]

Our group has previously reported the development of polymer–lipid hybrid nanotechnology, in which noncovalent drug–polymer complexes are efficiently encapsulated into a nanoscale core of mostly solid lipids.[23,24] Solid lipid ingredients in drug delivery platforms have been shown to extend the release profiles of diverse compounds and reduce their toxicity.[25–28] In a recent study, we further demonstrated that by introducing a small quantity of oil into the solid lipids of a hybrid system and tailoring their relative amounts, it was feasible to manipulate the nanoparticle internal structure and subsequently its drug release behaviors inside cancer cells.[29] As a result, controlled and sustained intracellular release kinetics was achievable.

In the present study, a lipid–PEI hybrid nanocarrier (LPN) incorporating linear PEI with hydrophobic, hexadecyl groups (hydrophobic hexadecylated polyethylenimine (H-PEI)) was developed and evaluated. We hypothesized that by integrating the controlled release and targeted delivery strategies, the resulting LPN technology would provide solutions or improvements to several key issues of siRNA/PEI systems in an "all-in-one" manner (see Figure 1a). This includes (1) physical encapsulation of the siRNA materials instead of just coating them on carrier surface, (2) reduction of the loss of siRNA to the extracellular environment but facilitation of controlled, sustained intracellular siRNA release, (3) prevention of quick exposure of the cells to a high level of unencapsulated PEI molecules, and (4) like other lipid carriers, providing sites for

TABLE 1. Size and Zeta Potential Measurements[a]

carrier	particle diameter (nm), mean ± SD: z-average value	PDI	zeta potential (mV), mean ± SD
blank PEI	2342 ± 1145	0.72 ± 0.28	+28.2 ± 1.2
siRNA-PEI polyplex	266.3 ± 70.6	0.62 ± 0.13[b]	+21.4 ± 5.7
blank H-PEI	70.7 ± 1.4	0.23 ± 0.01	+45.9 ± 4.5
siRNA-H-PEI polyplexes	312.2 ± 47.7[b]	0.65 ± 0.16[b]	+30.8 ± 8.3
LPN (no H-PEI, no siRNA)	145.8 ± 26.4	0.27 ± 0.07	−38.2 ± 4.3
LPN (with H-PEI, no siRNA)	155.0 ± 40.8	0.26 ± 0.01	−7.5 ± 7.2
LPN (with both H-PEI and siRNA)	213.5 ± 22.5[b]	0.25 ± 0.01[b]	−20.9 ± 8.3

[a] Particle size values presented were derived from distribution by intensity data. Mean of $N \geq 3$ samples were measured for each carrier type. PDI = polydispersity index. [b] $p < 0.05$ comparing unencapsulated siRNA-polyplexes to LPN with encapsulated H-PEI/siRNA.

easy surface-engineering (*e.g.*, grafting cell-targeting moieties).[30−33] These hypotheses were tested in both prostate cancer and noncancerous prostate cells with emphasis not only on the acute effects, but also on their delayed responses.

RESULTS

LPN Characterization. Table 1 and Figure 1 present the size data. After encapsulation of siRNA/H-PEI polyplexes (siRNA-H-PEI) to form LPNs, the mean size was slightly over 200 nm and the polydispersity index (PDI) was below 0.3, indicating good quality control over the carrier size distribution with the encapsulation approach. These values were both significantly smaller than the unencapsulated polyplexes ($p < 0.05$). Figure 1c presents the electron microscope images of LPNs (low and high magnification). Consistent with the photon correlation spectroscopy (PCS) data, the spherical LPNs shown in the image were mostly around 200−300 nm in diameter.

Table 1 also shows the zeta potential data. When the values of unencapsulated siRNA-H-PEI polyplexes, blank LPNs (without siRNA), and LPNs are compared, it is evident that the lipids bearing negative zeta potential (−38.2 mV) have screened out the positive charge of H-PEI/siRNA-H-PEI (+30.8 mV). As a result, the zeta potential of LPNs becomes mildly negative (−20.9 mV).

Figure 1d shows the pH response of LPNs. Overall, LPNs were physically stable in the pH range from 5 to 9. Particle aggregation started to appear at pH 4 or lower, as indicated by the increases in particle size and PDI values. This was likely due to changes in zeta potential at low pH values. In general, the aggregation was moderate. After 24 h incubation in pH 3, the particle size was around 340 nm.

siRNA encapsulation efficiency values of LPNs and nf-LPNs (LPNs without folate-PEG-DSPE (1,2-distearoyl-*sn*-glycero-3-phosphoethanolamine-*N*-[folate(polyethylene glycol)-2000])) were found to be 83.4 ± 6.2% and 85.3 ± 5.5 (mean ± SD, $n = 3$), respectively. The surface-modification did not significantly affect the siRNA encapsulation ($p > 0.05$).

Coating of Folate on LPNs Improved siRNA Uptake Efficiency and Selectivity for Folate-Receptor Expressing Cancer Cells. Figure 2 shows the effects of different carrier systems on the siRNA uptake by folate-receptor expressing PC3 cancer cells (Figure 2a) and folate-receptor deficient noncancerous RWPE1 cells (Figure 2b) as measured by flow cytometry. Trypan blue quenching was performed to eliminate the extracellular fluorescence so the measured fluorescence was from the siRNA within the cells. In PC3 cells, the standard, folate-coated LPNs (LPN, black bar) delivered siRNA at comparable or better rate than Lipofectamine 2000 (Lf), conventional PEI, or H-PEI. This high siRNA transfection rate was significantly reduced in LPNs without folate modifications (nf-LPN) or when LPN uptake was partially blocked by a high folate level (++folate, also black bar). This indicated that the LPN uptake into PC3 cells was largely receptor-mediated. This was supported by the RWPE1 data. In these cells, both LPNs and nf-LPNs could no longer rely on the folate-receptor pathway. Consequently, they both demonstrated lower siRNA uptake than Lf, PEI, and H-PEI. It should be pointed out that the uptake rates of all carrier types by RWPE1 cells were generally lower than PC3 cells. A few % reduction in siRNA transfection by Lf, PEI, H-PEI and nf-LPNs was observed in each group. These modest cell-type related differences, however, cannot explain the substantial reduction of LPN-mediated siRNA transfection by RWPE1 cells (from 88% to 21% transfection, $p < 0.05$). This can only be explained by the cancer-targeting ability of the folate-coated LPN design.

As a supplementary method, the cellular siRNA uptake was also measured by fluorescence microplate reader (Figure S1, see Supporting Information). A similar trend was observed.

The fact that regardless of the method used, modest LPN uptake remained detectable in RWPE1 cells indicates that some extent of nonspecific uptake was still in effect. The carrier-cell interaction was diminished probably as a result of the more negative zeta potential value of LPNs, and this was compensated by the receptor-mediated uptake in PC3 cells. Overall, the

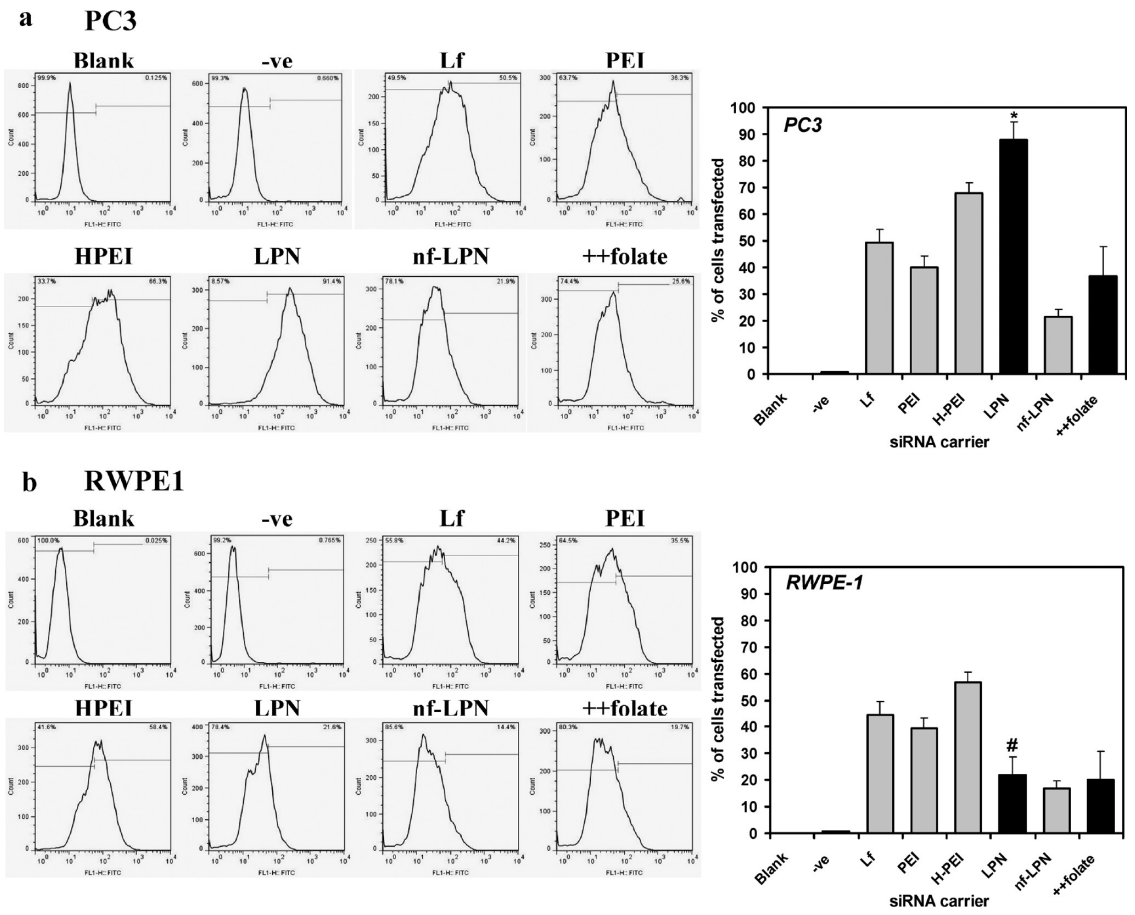

Figure 2. Flow cytometry measurement of the siRNA transfection efficiency of different carriers. (a) Cancerous, folate-receptor expressing PC3 cells and (b) noncancerous, folate-receptor negative RWPE1 cells were transfected with siRNA using different carriers, followed by trypan blue quenching before flow cytometry measurement. Negative controls include untreated cells (Blank) and cells treated with LPNs carrying non-fluorescent, inactive siRNA (-ve). Treatments include 50 nM FAM-siRNA delivered by different carriers including Lipofectamine-2000 (Lf), linear PEI (PEI), PEI grafted with hydrophobic hexadecyl groups (H-PEI), regular LPNs (LPN) and LPNs without folate-linked moieties (nf-LPN). A group was treated with LPNs in the presence of a high folic acid level (0.1 mM) to block the folate receptor (++folate). Left panels present the histogram data (*y*-axis: cell count; *x*-axis: fluorescence intensity using FL1/FITC channel) and right panels present the % of cells successfully transfected after treatment (20,000 cells per measurement, $n = 3$ and mean ± SD presented). * $p < 0.05$ comparing LPN group to all other groups; # $p < 0.05$ comparing LPN group to Lf, PEI and H-PEI but no significant difference comparing to nf-LPN and ++folate.

data demonstrated a simultaneous reduction in the nonspecific siRNA uptake and increase in the cell-specific, receptor-mediated uptake when siRNA was delivered using folate-coated LPNs. These two trends worked in combination to effectively improve the siRNA transfection efficiency and selectivity for the targeted cancer cells.

LPNs Reduced Extracellular Loss of siRNA. siRNA molecules that prematurely release from the carrier before transfection generally do not transfect well. This issue was investigated by studying the siRNA release in a buffered medium at 37 °C (Figure 3a). Comparison of the full profiles showed significantly less loss of siRNA into the medium from LPNs than the two conventional PEI formulations (One-way ANOVA: $p < 0.05$). As substantial transfection should have occurred within the first few hours, we highlighted the earlier measurements in the first 5 h (in the small chart). After 4 h, PEI, and H-PEI lost 35% and 29% of their siRNA, respectively, significantly more than the 14% loss from LPNs ($p < 0.05$). The data indicate reduced loss of siRNA from LPNs to the medium especially by initial burst releases.

siRNA molecules in their carriers may also be physically lost or degraded during storage. Figure 3b shows the % of siRNA remained in LPNs after incubation at different conditions. 100 h storage at high temperature in medium or 5% dextrose tends resulted in modest loss (17−35%) of siRNA. siRNA in the lyophilized samples were generally well retained in LPNs.

LPNs Extended Intracellular siRNA Release. Flow cytometry measurements of the decline of 5-FAM-siRNA levels in PC3 cells (2 days to 7 days after transfection) are shown in Figure 4a. Two days after transfection, LPN group showed the highest intracellular siRNA level. However, the difference between LPN group and H-PEI group was not significant at that point. Seven days after transfection, the siRNA level in the LPN-treated cells was significantly higher than all other groups.

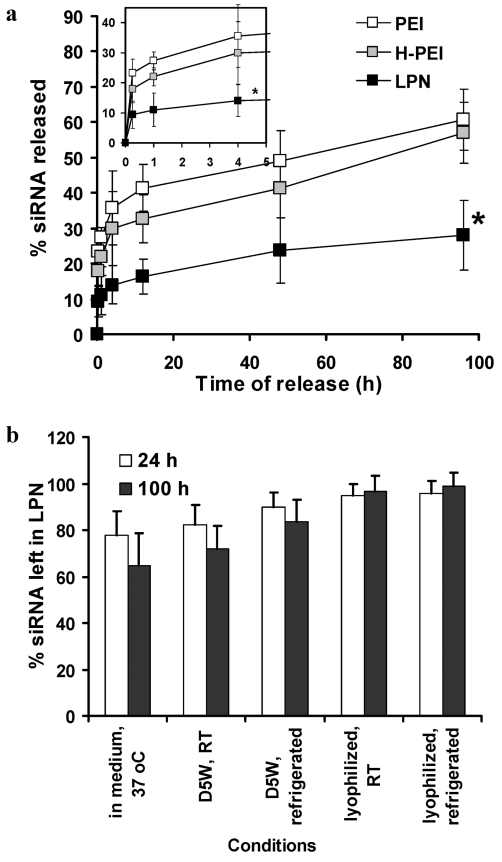

Figure 3. LPNs reduce the extracellular loss of siRNA. (a) Fraction of siRNA released from carriers, including linear 2500 Da PEI (PEI), PEI grafted with hydrophobic hexadecyl groups (H-PEI) and LPN, in colorless RPMI 1640 medium supplemented with 10% phosphate buffered saline (pH = 7.4) at 37 °C. The main chart presents the whole release profiles in 96 h, while the small chart within magnifies the first 5 h portion to highlight the initial burst releases. *Indicates significant differences ($p < 0.05$, $n = 3$) between LPN and other groups at the same time point. (b) Stability study of LPNs: The quantities of siRNA remained in LPNs after storing them at different conditions are normalized against the same amount of freshly made samples and presented as means S. ($n = 3$). Medium: colorless RPMI 1640 medium/PBS (90:10 v/v), D5W: 5% dextrose in water, refrigerated: 4 °C, RT: room temperature or 25 °C.

Approximately 30% cells still contained high siRNA level. In comparison, less than 10% cells transfected by Lipofectamine (Lf), PEI, or H-PEI had significant intracellular level of siRNA. Interestingly, although the initial siRNA level in the nf-LPN group was only around 20%, less than half when comparing to the H-PEI group on day 2, it became higher than all other groups except LPN on day 7. All these flow cytometry findings are consistent with the fluorescence images presented in Figure 4b. Similar to the standard LPNs, a visibly detectable level of siRNA persisted on day 7 in nf-LPN group. This suggests that even though the cellular uptake was diminished by eliminating the receptor mediated uptake, the sustained intracellular release feature was preserved in nf-LPNs.

LPNs Exhibited Reduced Acute and Delayed Carrier Toxicity. Figure 5 presents the results of four assays comparing the acute and delayed cellular toxicity of LPNs to PEI and H-PEI systems (all carrying inactive siRNA). The responses of the noncancerous RWPE1 and cancerous PC3 cells are reported. As the solid lipid and phospholipid components of LPN are substantially less toxic than cationic materials,[28,29,34] we focused on comparing the carriers on the basis of the amount of PEI fraction instead of the whole carrier. Figure 5a presents the membrane integrity data measured by lactate dehydrogenase (LDH) assay. High level of LDH leakage into the culture medium indicated cell membrane damages subsequent to the cell exposure to PEI. It was shown that significantly less cell membrane damages were inflicted by LPNs at the same PEI dosing level ($p < 0.05$, one-way ANOVA). This translated into better short-term cell viability (Figure 5b) measured with trypan blue assay, as demonstrated by the highest LD50 values LPN groups. The acute carrier toxicity to both cell types was mitigated by the use of LPNs.

The delayed toxicity was evaluated with MTT assay and clonogenic assay. Figure 5c presents the MTT assay results. Two dosing levels (1 and 5 μg/mL PEI) were tested. We selected these two levels because they did not cause strong acute toxicity (<10% LDH leakage in Figure 5a, >90% viability in Figure 5b) so we could focus on the delayed component. At a high dosing level, LPNs were significantly less toxic to both cell types, but at a lower dosing level, LPNs were significantly less toxic to RWPE1 only. This trend persisted in the result of clonogenic assay (Figure 5d) which measures the cell proliferation capability. RWPE1 cells remained substantially more proliferative after LPN treatment than the other two groups especially after 5 μg/mL treatment. After normalization, 73% of LPN-treated RWPE1 cells were able to form colonies compared to only 29% of H-PEI treated cells. LPN was still less toxic, albeit not statistically significant, to the PC3 cells when compared to the conventional PEI groups after 5 μg/mL treatment. Overall, LPN was able to mitigate both the acute and delayed toxicity. The reduction in the delayed toxicity to the noncancerous RWPE1 cells was particularly strong.

An nf-LPN group was included in the colony formation assay to evaluate the effect of cell-targeting on cell toxicity (Figure 5d). Significant difference in colony formation rates between the standard, folate-coated LPNs and nf-LPNs was observed in PC3 but not RWPE1 cells. This indicates that the reduced toxicity of LPNs in RWPE1 cells is at least in part due to their lower expression of folate receptors and thus the decreased uptake of the folate-coated LPNs.

LPNs Increase Duration of the Effects of siRNA on mRNA Expression and Survivin Knockdown. Figure 6 panels a and b show the extended *in vitro* knockdown effects of siRNA-loaded LPNs on mRNA expression and protein level. Survivin served as the model target in these studies. In Figure 6a, only LPNs carrying survivin-targeting siRNA

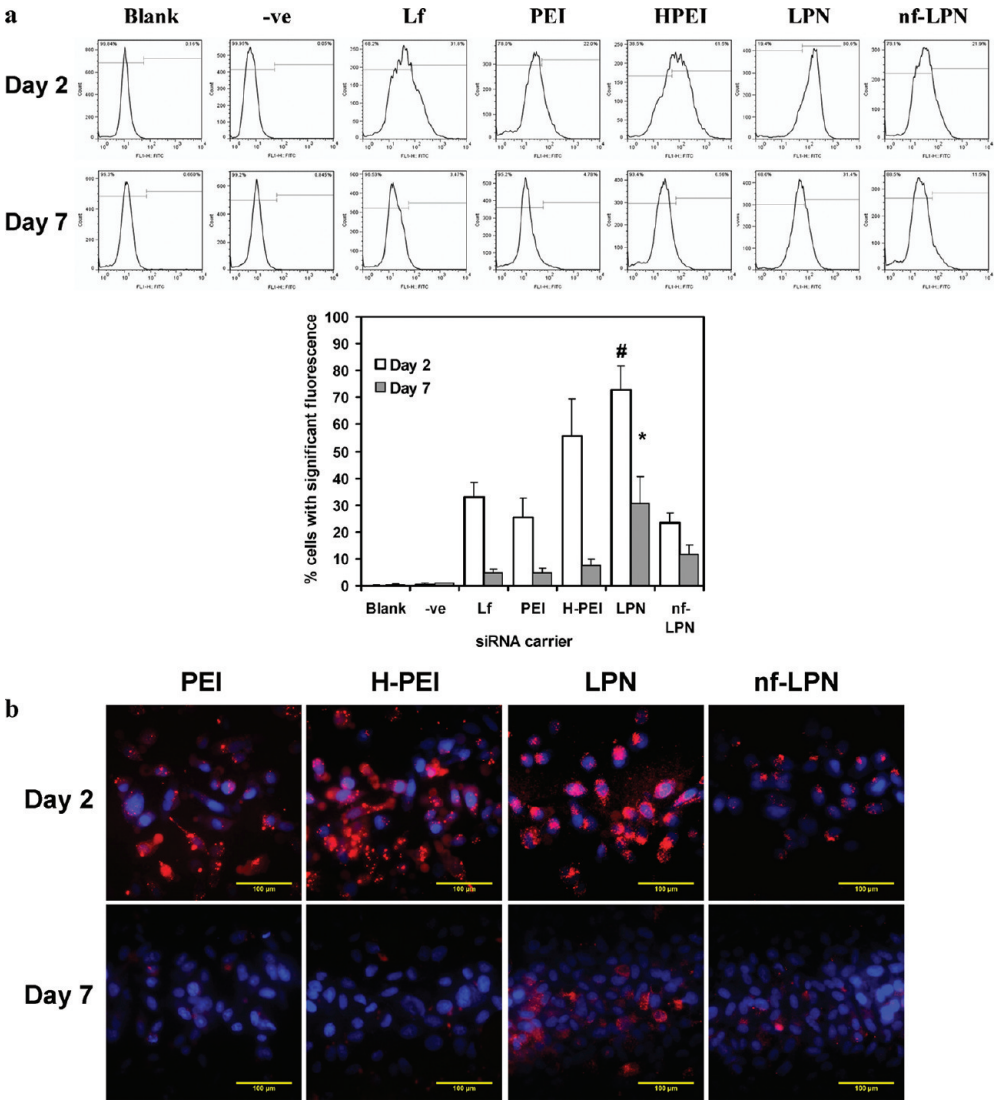

Figure 4. LPNs extend the intracellular siRNA release. (a) Flow cytometry measurement of the decline of FAM-siRNA level in PC3 cells from 2 days to 7 days after transfection. Upper panel presents the histogram data (*y*-axis: cell count; *x*-axis: fluorescence intensity using FL1/FITC channel) and lower panel presents the % of cells containing significant level of siRNA (20,000 cells per measurement, $n = 3$, mean $\pm$ SD presented). # $p < 0.05$ comparing LPN to all other groups except H-PEI; * $p < 0.05$ comparing LPN to all other groups. (b) Fluorescence microscope images of PC3 cells comparing the intracellular kinetics of rhodamine-siRNA delivered by different PEI carriers including PEI, H-PEI, LPNs and LPNs without folate (nf-LPN) on day 2 or 7 after transfection. Red fluorescence indicates siRNA and far red (as blue pseudo-color) indicates the cell nuclei stained by DRAQ5 nuclear dye. Scale = 100 m.

(survivin-siRNA) maintained strong suppression on the survivin mRNA (to around 20% of the control) on day 7. In Figure 6b, the *in vitro* survivin knockdown effect of LPNs was found to last for 7 days, versus 3−5 days in the H-PEI group. This agrees with the imaging result presented in Figure 4b and shows that the sustained intracellular presence of siRNA could translate into extended *in vitro* RNAi activity. LPNs carrying inactive siRNA (-ve group) were included in both experiments. No significant effect on survivin mRNA and protein levels was observed. The carrier effect was thus ruled out.

LPNs Carrying Survivin-siRNA Provide Significant, Extended *in Vivo* RNAi Activity. Figure 7a compares the survivin levels in PC3 tumors after intravenous administration with different carriers loaded with survivin-siRNA. The original images (left) and the corresponding images of brownness (indicating the survivin level) extracted using ImageJ software (right) are shown. The tumor survivin levels remained significantly suppressed (*i.e.*, reduction in brownness) to day 7 in the LPN group. In comparison, modest survivin knockdown effect was noticed in the H-PEI group on day 2, but this effect quickly wore off on day 7. Figure 7b shows the tumor size measurements. Significant tumor growth suppression was observed comparing the LPN to all other groups ($p < 0.05$). It should be pointed out that although survivin has a direct antitumor effect, its key strength lies in its broad-spectrum chemosensitization effect (please see Discussion), so the tumor growth suppression was only moderate. Figure 7c presents the body weight data.

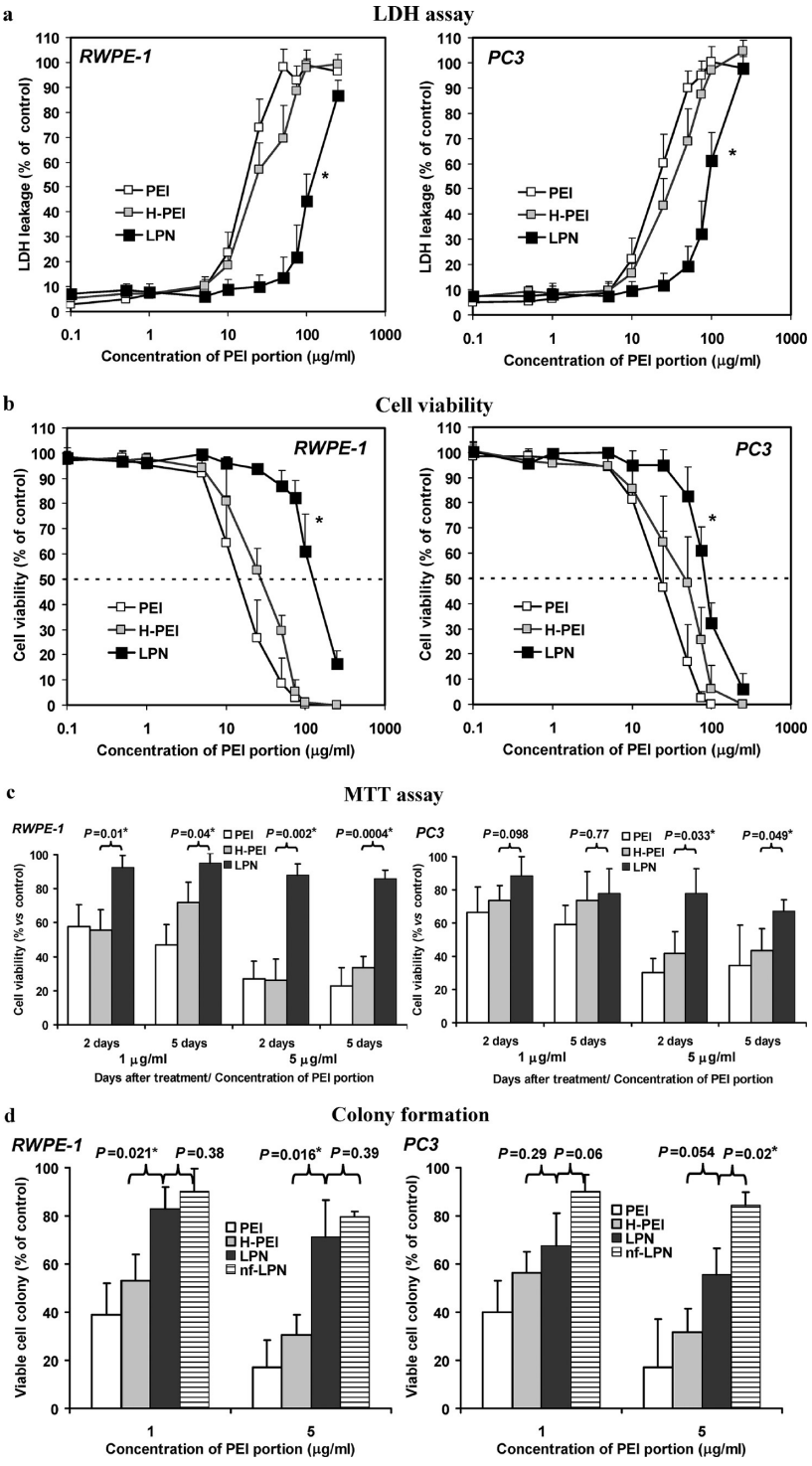

Figure 5. Comparison of the carrier toxicities of LPN to other PEI-based systems. (a) LDH assay to determine the cell membrane integrity after treatment. Treatments including unmodified, linear 2500 Da PEI (PEI), PEI grafted with hydrophobic hexadecyl groups (H-PEI) and LPN. They were tested on the noncancerous RWPE1 cells (left panel) and cancerous PC3 cells (right panel). Results are normalized against the vehicle control (5% dextrose, as baseline) and 1 mg/mL PEI (positive control, as 100%). Mean + SD ($n = 3$) are presented. (b) Trypan blue assay to evaluate cell viability as a function of the acute carrier toxicity. Conditions used were same as (a). The dotted line in each graph intersects the 50% viability. LD50 values of PEI, H-PEI and LPN groups were found to be 15, 55, and 120 g/mL in RWPE1 cells and 24, 45 and 87 g/mL in PC3 cells, respectively. (c) MTT assay to evaluate the delayed toxicity on RWPE1 (left panel) and PC3 cells (right panel) 2 or 5 days after treatment. Results are normalized against the corresponding vehicle control group (as 100% viable), and mean + SD are presented ($n = 3$). LPN and H-PEI groups were compared and p values were shown. (d) Clonogenic assay to evaluate the delayed effects of carriers on cell proliferation in a longer-term. Results are normalized against the corresponding vehicle control group (as 100% viable colony formation), and mean + SD are presented ($n = 3$). An non-folate receptor targeting LPN group (nf-LPN) was included to evaluate the role of targeted delivery feature in toxicity reduction. In all figures, * represents significant difference ($p < 0.05$, one-way ANOVA used for (a) and (b), two-tailed Student's t-test for (c) and (d)).

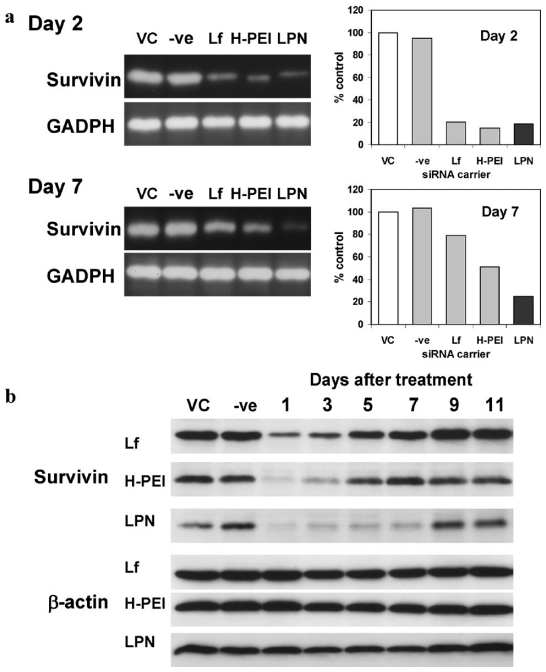

Figure 6. LPN increases the duration of the effects of siRNA on (a) mRNA expression (b) survivin knockdown. (a) Relative survivin mRNA expression in PC3 cells two or seven days after siRNA treatment was determined by RT-PCR. 50 nM survivin-siRNA was delivered by different carriers (Lf: Lipofectamine-2000, H-PEI: hexadecyl PEI, and LPN). Negative controls include vehicle control (VC, blank medium, first lane from left) and LPN carrying inactive siRNA control (-ve, second lane from left). GADPH was used as an internal control. Right panel presents the relative expression normalized against the VC group. (b) The effect of carriers on the time profiles of survivin knockdown was evaluated by Western immunoblotting. The survivin levels from Day 1 to Day 11 after transfection were monitored and compared. Treatments and controls are the same as (a). Cells in the VC and "-ve" groups were harvested three days after transfection. β-actin was used as the total protein loading control.

All groups lost less than 10% body weight after treatment. Both LPN groups (LPN, LPNs carrying survivin-siRNA; -ve, LPNs carrying inactive siRNA) did not cause significantly higher body weight when compared to the vehicle control (VC).

DISCUSSION

PEI is a nonviral gene delivery material of vast potential. However, the conventional approaches of utilizing PEI clearly have substantial room for further development. Currently, polyplexes are typically prepared by freely complexing nucleic acids with PEI molecules or preformed PEI-based systems. There is a general lack of effective means to control the behaviors of their payload release, limit their nonspecific interaction and toxicity with the healthy tissues, and equip the polyplexes for more favorable biodistribution. We thus proposed to simultaneously overcome these multiple limitations by integrating the controlled release properties of a solid lipid based platform with a receptor-targeting strategy in the form of LPN technology.

Recently, researchers have increasingly realized the advantages of adding lipid or phospholipid components to PEI. Two strategies are often adopted. The first strategy relies on direct lipidation of PEI and using the modified PEI for direct siRNA delivery,[16,21,35] and the second one involves combining preformed siRNA/PEI polyplexes with phospholipids to form PEI-liposomes.[20,36] Direct lipidation of PEI was shown to significantly reduce the degradation of bound siRNA.[35] The findings on the more sophisticated PEI-liposomes, or lipopolyplexes, are even more interesting. It was shown that the biological properties of these lipopolyplexes are primarily determined by the liposome shell.[36] In other words, the choice of the lipids may serve as the key to control the siRNA/PEI behaviors, overcome their limitations, and even improve their performance. This is in support of the general theme of LPN technology.

Solid lipids have been shown to provide a stable yet biodegradable and biocompatible diffusion barrier to protect diverse encapsulated compounds and control their release.[24−29] This controlled release feature was exploited here for three potential benefits. First, the premature release of siRNA could be reduced. Figure 3a shows significantly less siRNA dissociated from LPNs into the buffered medium when compared to the two unencapsulated PEI groups. Figure 3b shows that the siRNA molecules loaded in LPNs remained mostly encapsulated during extended storage. Literature[6,37,38] and our uptake data in Figure S1 (see Supporting Information) have demonstrated the low transfection efficiency and poor *in vitro* and *in vivo* stability of free, released siRNA molecules. By encapsulating siRNA molecules in lipids to reduce premature release, it is expected to improve the efficiency of their usage to start with.

Dye-binding (RiboGreen) method was used for evaluation of extracellular siRNA release from LPNs in this study. This is a well-established method to evaluate the dissociation of siRNA molecules from their carriers.[39] However, this method is limited for measurement of free siRNA in the absence or at low level of serum, as in the case of the current study. In the presence of serum such as in systemic circulation, the loss of siRNA from the carrier is expected to be even faster as the binding of charged serum may dissemble the siRNA-carrier complexes.[40] The role of the carrier to protect its load of siRNA before reaching the disease site thus becomes even more critical. As a result, the advantage of LPNs could turn out to be more obvious. To test this hypothesis, a more sophisticated method such as fluorescence fluctuation spectroscopy, which is able to measure the integrity of siRNA-carrier complexes in full human serum, can be applied.[41] This issue will be investigated in our future studies.

Second, we hypothesized that LPNs will also help siRNA to stay inside the cells for longer time after transfection. Figure 4 demonstrates this short intracellular lifespan of siRNA when delivered by the unencapsulated

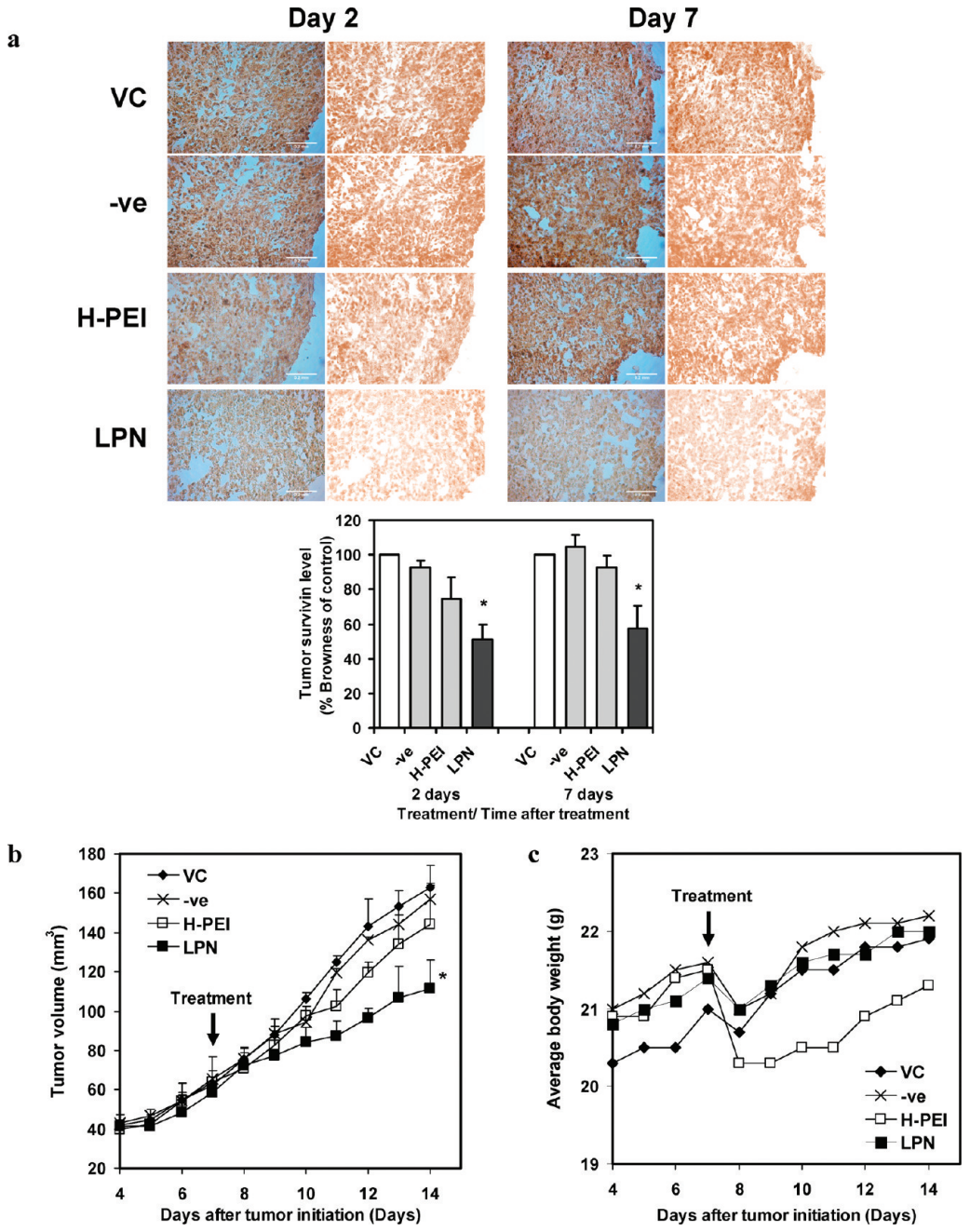

Figure 7. LPNs carrying survivin-siRNA provide significant, extended *in vivo* RNAi activity. (a) Immunohistochemical staining of PC3 tumors each treated with 0.5 nmol of survivin-siRNA carried by H-PEI or LPNs by tail-vein injection. VC (Vehicle control) group and "-ve" group were treated with 5% dextrose for injection and LPNs carrying 0.5 nmol of inactive siRNA, respectively. Upper panel presents the immunohistochemically stained tumor sections and the corresponding images of their "brownness" (indicating the survivin level). Lower panel presents the image analysis data indicating the normalized tumor survivin levels (mean + SD, $n = 3$, VC as 100%). (b) and (c) Time profiles of average tumor volume and body weight of animals (means + SD for (b), SD not shown in (c) for clarity. $n = 3$ per group). Arrow in each graph indicates the time of treatment. * $p < 0.05$ comparing LPN to other groups.

PEI systems (PEI and H-PEI). The cellular siRNA levels rapidly declined and became barely detectable on day 7. In comparison, LPNs were able to prolong the intracellular presence of siRNA to ≥7 days. The detailed mechanism underlying this sustained siRNA release still warrants further investigation. Our previous studies of the intracellular behaviors of solid lipid-based carriers indicate that this is, at least in part, attributable to the controlled degradation of the solid lipid components by the intracellular enzymes (*e.g.*, lysosomal acid lipase).[29] An internalized nanoparticle with a relatively firm structure due to the high content of high melting point lipids tends to respond slowly to the enzymatic activities. In the case of LPNs, this could lead to gradual release of its siRNA payload to the cell content, so they effectively served as a long-acting intracellular source of siRNA.

As a third benefit, in addition to the siRNA, H-PEI was also encapsulated in LPNs. This prompted us to hypothesize that the controlled release feature would prevent direct exposure of the cells to a full dose of the fairly toxic PEI molecules. PEI was previously shown to cause both acute toxicity and delayed toxicity.[10,42] Figure 5 panels a and b show that LPNs are effective in reducing the nonspecific, acute cellular toxicity. Decreases in the membrane damage and improvements of cell viability by several folds were observed in the LPN group, especially in the range used for high dose transfection (5−50 μg/mL PEI). The toxicity reduction effect of LPNs was more noticeable in RWPE1 than PC3 probably because the targeting feature of LPN only applied to PC3 cells, as reflected by the further reduction in toxicity of nf-LPNs to PC3 cells only (see Figure 5d). Nevertheless, LPNs still caused considerably less acute toxicity in the PC3 cells than the two PEI polyplexes even they were taken up by the cells at a comparable or higher rate (Figure 2). This further highlighted the toxicity reduction function of the lipids in LPNs.

Given all the benefits associated with the controlled release feature of LPNs, we also noted that this strategy was associated with a number of potential issues. First, we were concerned that the strategy of gradually exposing the cells to H-PEI, while lessening the acute carrier toxicity, would exacerbate the delayed toxicity component. This was ruled out by the data of MTT assay (Figure 5c) and clonogenic assay (Figure 5d), which measured the delayed cell death (day 2 and 5) and cell proliferation (>10 days), respectively. Instead of increasing the delayed toxicity, the data showed that LPNs remained relatively less toxic in a longer term especially to the noncancerous RWPE1 cells. We therefore conclude that the cells are able to handle a low, sustained level of the PEI molecules that gradually become free from the lipids.

The second issue concerned whether the siRNA molecules delivered by LPNs would remain intact and biologically functional, or were simply trapped in the LPNs. Using a highly expressed protein survivin as the model target, our data in Figure 6 and 7 demonstrated that the survivin-siRNA in LPNs preserved their functionality, and the sustained intracellular siRNA release was translatable into *in vitro* and *in vivo* extended RNAi activities. The duration of survivin knockdown was approximately doubled. It should be noted that survivin is a clinically valuable target. Its knockdown was found to sensitize several drug-resistant cancers (*e.g.*, prostate cancer) to chemotherapy compounds.[43,44] By expanding the time-window of survivin knockdown, the LPN-treated cancer will be in a sensitive state to chemotherapy for considerably longer time, which is therapeutically desirable considering that the anticancer effects of many chemotherapy drugs (*e.g.*, docetaxel for prostate cancer) are time-dependent.[45]

Our third concern derived from the weakened nonspecific carrier-cell interactions. The positive charges of the physically encapsulated PEI molecules were hidden by the lipids (Table 1). This would potentially compromise the transfection performance. The diminished siRNA uptakes in the nf-LPN group in Figure 2 *versus* the two PEI-polyplexes showed that this was a legitimate concern. We addressed this issue by integrating a receptor-targeting strategy for cell-specific uptake. The lipids of LPNs provide ample convenient sites for grafting targeting moieties to exploit the receptor-mediated endocytosis pathways. Using folate-receptor as a model target and folate-tagged lipids as the targeting agent, our data of siRNA uptake (Figure 2) and microscope imaging (Figure 4b) both show that the receptor-mediated uptake is sufficient to compensate for the diminished nonspecific component in cancer cells, and this is beneficial as the interaction between the carrier and noncancerous cells is reduced and so is the nonspecific toxicity (Figure 5). In effect, the targeted delivery strategy has covered the most critical concern of the controlled release strategy by shifting the PEI-mediated siRNA transfection from a predominantly nonspecific event to a cell-specific one. Here we demonstrated that these two strategies complement each other and should be implemented in an integrated fashion.

Finally, Table 1 shows that LPNs are significantly smaller and less polydispersed than the uncoated siRNA-PEI and siRNA-H-PEI polyplexes, which are over 250 nm in diameter with high PDI. This finding is in apparent contradiction to the recent studies of siRNA-PEI by Kostka *et al*. and Mao *et al*.,[46,47] which both reported smaller size (in the range of 120−150 nm) of the formed polyplexes with low polydispersity. This discrepancy is probably attributable to the differences in the materials used and the preparation conditions. In those studies, PEI molecules were tagged with hydrophilic components such as *N*-(2-hydroxypropyl)methacrylamide copolymer or PEG. This may stabilize the formed polyplexes and prevent their aggregation. Additional steps such as filtration of the complexes over 0.22 μm PVDF filters presaturated with PEI were also included to further improve their size control.[46] It should be noted that the larger size of the siRNA-H-PEI used in the present studies may have adversely affected their uptake by cells. One must therefore keep in mind that there are other PEI modification approaches other than lipidation and lipid encapsulation to control the size and increase the performance of siRNA−PEI polyplexes. The key strength of the LPN technology remains to be overcoming multiple limitations of siRNA and cationic polymers in a convenient, well-integrated fashion.

CONCLUSIONS

This study reports an all-in-one, nanomedicine-based approach to overcome multiple key limitations of the

promising siRNA–PEI therapy. By exploiting the strengths of the polymer–lipid hybrid nanotechnology and complementing their potential weakness with a cell-targeting strategy, the new form of RNAi treatment is more efficient, extended, target-specific, and likely safer to be implemented. Our next study will investigate the *in vivo* fate of LPNs and optimize their pharmacokinetics to further increase their translational potential. It must be noted that while the molecular target (survivin) and cell surface target (folate-receptor) both have significant therapeutic values for cancer treatment, the present study is primarily for proof-of-concept of the proposed integrated approach. The same concept should be applicable to diseases other than prostate cancer by carefully choosing the molecular and cell-surface targets. The extended release and toxicity reduction features of LPNs are particularly suitable for the treatment of chronic disease conditions. Future studies will further explore these possibilities and understand the implications of this new approach.

EXPERIMENTAL SECTIONS

Selection of Model siRNA, Molecular Target, and Cell Surface Target. Four model siRNAs were chosen to achieve our various objectives. Rhodamine-siRNA and FAM-siRNA both carry a fluorescent group on the sense strand of a nonsilencing control siRNA duplex. It was used for microscope imaging and flow cytometry measurement of the intracellular siRNA. Negative-siRNA served as an inactive "filler" in carriers for carrier toxicity studies and as a negative control for immunoblotting studies. We selected nontargeting siControl #3 for these purposes because of its minimal effects on cell viability and survivin expression.[29,37] Survivin-siRNA was selected for evaluation of the RNAi functionality. We chose survivin and folate receptor as the molecular target of siRNA and cell surface target, respectively, because both are documented to express at elevated levels in a majority of human cancers including PC3.[43,48,49] Survivin also has quick turnover (2–4 h) so the time effect of LPNs could be clearly demonstrated.[50] In addition, survivin knockdown can be used to restore cancer chemosensitivity, while folate-receptor is poorly expressed in noncancer cells such as RWPE1.[44,49,51] Hence, the LPNs made for these targets also have application potential besides serving as model targets.

Chemicals and Reagents. Rhodamine-siRNA (rhodamine-conjugated All-Stars siRNA, 5′-UUCUCCGAACGUGUCACGUdTdT-3′) was ordered from Qiagen (Valencia, CA). Survivin-siRNA (Human BIRC-5 ON-TARGET duplex siRNA targeting survivin, 5′-P-UCUGGCUCGUUCUCAGUGGUU-3′) and negative-siRNA (nontargeting siControl #3, 5′-AUGUAUUGGCCUGUAUUAG-3′) were purchased from Dharmacon (Chicago, IL).

Linear PEI (2500 Da) was purchased from Polysciences (Warrington, PA), dissolved in dichloromethane–methanol (4:1 v/v), filtered, and lyophilized before use. Tripalmitin and triolein were purchased from TCI America Chemicals (Boston, MA). 1,2-Distearoyl-*sn*-glycero-3-phosphoethanolamine-*N*-[folate(polyethylene glycol)-2000] (DSPE-PEG-folate), 1,2-distearoyl-*sn*-glycero-3-phosphoethanolamine-*N*-[methoxy-(polyethylene glycol)-2000] (DSPE-PEG), 1,2-distearoyl-*sn*-glycero-3-phosphoethanolamine (DSPE), cholesterol, and the green-fluorescent phospholipid 1,2-dipalmitoyl-*sn*-glycero-3-phosphoethanolamine-*N*-(7-nitro-2-1,3-benzoxadiazol-4-yl) (NBD-PE) were obtained from Avanti Polar Lipids (Alabaster, AL). RiboGreen RNA Quantitation Reagent was obtained from Invitrogen (Carlsbad, CA), DRAQ5 dye was from Biostatus (Leicestershire, UK), antibodies were from Santa Cruz (Santa Cruz, CA), and other chemicals were from Sigma-Aldrich (St. Louis, MO).

Cell Cultures. Noncancerous RWPE1 human epithelial cell line and human prostate cancer PC3 cell line were purchased from American Type Culture Collection (Manassas, VA). RWPE1 cells were maintained in Defined Keratinocyte Serum Free Medium (Invitrogen/GIBCO, Grand Island, NY) supplemented with the human recombinant epidermal growth factor. PC3 cells were cultivated in colorless RPMI 1640 medium supplemented with 10% fetal bovine serum, 50000 units penicillin G, and 50000 μg streptomycin. Both cell lines were incubated at standard cell culture conditions (37 °C, humidified atmosphere of 5% CO_2 in air). Cells were passaged every 5–7 days and used for experiments from 10th to 25th passages.

Animals and Tumor Model Preparation. Male athymic mice at 5–6 weeks old were purchased and acclimatized for 7 days before use. For tumor model preparation, subconfluent PC3 cells were harvested, suspended in cell culture medium, and mixed with Matrigel (Becton Dickinson, Bedford, MA) in a 1:1 ratio, and 100 μL of the mixture containing 2×10^6 cells were injected subcutaneously at the back flank area of each mouse to initiate tumor growth. Animals were cared for in accordance with institutional guidelines and had access to food water *ad libitum*.

Hydrophobic Modification of Linear PEI. Hexadecyl groups were grafted on linear PEI to form hydrophobic, hexadecylated PEI (H-PEI) for LPN preparation. The substitution reaction was conducted based on the method of Masotti A., *et al.*[20] modified for linear PEI. 1-Bromohexadecane (0.945 g) in 50 mL of dichloromethane was added over a period of 3 h to a solution of PEI (1 g) and triethylamine (1 mL) in 100 mL of dichloromethane/methanol (95:5 v/v). The resulting mixture was stirred at room temperature for 48 h and concentrated to 20 mL under vacuum. The product was purified by dialysis against 50% ethanol (5 cycles × 1 L) followed by RNAase free water, adjusted to pH 4–5, and lyophilized before use. ^{1}H NMR spectrum of the solution of H-PEI in $CDCl_3$ was recorded on a 400 MHz Bruker Biospin instrument (Billerica, MA). Peaks found include δ (ppm) 0.86 ($-CH_3$), 1.26 ($-(CH_2)_{14}-$), 2.65 ($-CH_2CH_2N-$), 3.41 ($-CH_2-$) (see Supporting Information, Figure S2). The substituted product is represented by the stoichiometric formula $(C_2H_4N)_{59}(C_{16}H_{33})_{59n}$, where 59 is the average number of the ethylenimine units and n is the % of ethylenimine units with substitution. The NMR result showed that n was 11.8% (13% if substitution complete). No residue solvent peak was detected

Nanocarrier Preparation. LPNs were prepared using solvent evaporation technique as follows. A 15 nmol portion of siRNA was precomplexed with 0.7 mg H-PEI in a chloroform solution containing 2 mg triolein. This resulted in an N/P ratio of 15:1, which was previously shown to provide good transfection efficiency without strong toxicity.[11] In our screening study (Figure S3, see Supporting Information), near maximum siRNA/H-PEI complexation was obtained at this ratio. Since further improvement in siRNA binding was not observed at higher N/P ratios, and high N/P ratio often increases toxicity, we decided to use this ratio (*i.e.*, 15:1). The solvent was removed in vacuum and the siRNA-H–PEI–oil mixture was dissolved in 0.4 mL of dichloromethane solution of solid lipids including 6.5 μmol (2.5 mg) of cholesterol, 1.88 μmol (1.5 mg) of tripalmitin and 3.33 μmol (2.5 mg) of DSPE, and lipids for surface modifications including 0.5 μmol (1.3 mg) of DSPE-PEG and 0.05 μmol (0.2 mg) of DSPE-PEG-folate. DSPE-PEG-folate was replaced with DSPE-PEG in nontargeting LPNs. Nanocarriers were formed by dispersing the mixture in 3 mL of 5% dextrose solution containing 0.1% w/v soy lecithin by sonication for 3 min (40kHz, 120 V, Bransonic 3510, Danbury, CT) followed by stirring at 1200 rpm in vacuum at room temperature.

Conventional PEI polyplexes of siRNA were prepared by the direct complexation method.[18] Thin films of PEI or H-PEI were sonicated in 5% dextrose for 3 min to form polymer suspension. Polyplexes were formed by incubating the dispersed polymer

with siRNA at room temperature for 20 min at an N/P ratio of 15:1.

Size Distribution and Zeta Potentials. Particle size and zeta potential values were measured using photon correlation spectroscopy using Malvern Zetasizer NanoZS90 (Worcestershire, UK) at 25 °C. For each measurement, 50 μg (for size) or 100 μg (for zeta potential) of sample of nanocarriers was dispersed in 2 mL of distilled water and 15 successive cycles were run.

pH Response Study. A 500 μg aliquot of sample of LPNs was dispersed in 15 mL of buffer solution with pH value ranging from 4 to 9. The mixture was incubated at 37 °C under magnetic stirring. At specified time points (1, 8, 24 h), a 2 mL aliquot was drawn for size distribution and zeta potential measurement as described above.

Scanning Electron Microscopy. Particle morphology was examined using a scanning electron microscope (Jeol 7500F SEM). An aqueous suspension of LPNs was spread on a cover glass #1 and dried overnight in a desiccator. The cover glass was mounted on a carbon tape and sputter-coated with a thin gold−palladium (60:40) layer under an argon atmosphere, and scanned at an acceleration voltage of 5−15 kV.

siRNA Encapsulation Efficiency. A 2 μL aliquot of freshly prepared nanocarrier sample containing 0.01 nmol total siRNA was diluted to 30 μL with PBS (pH 7.4) in a 96-well microplate, and was incubated with 100 μL RiboGreen (prediluted by 1000−2000X) in Tris-EDTA buffer (10 mM Tris-HCl, 1 mM EDTA, pH 7.4 in RNAase free water) at room temperature for 2 min. Fluorescence was measured with SpectroMax microplate reader ($\lambda_{ex}/\lambda_{em}$: 485 nm/530 nm). The amounts of unencapsulated siRNA were quantified by comparison to a standard curve prepared from mixing 6.67 μg of blank nanocarriers with free siRNA solution at different concentrations.

Flow Cytometry Measurement. The effects of carriers on the transfection efficiency and intracellular siRNA kinetics were evaluated by flow cytometry with trypan blue quenching technique in accordance with previous studies.[52] For transfection efficiency measurement, PC3 or RWPE1 cells were treated with different carriers loading 50 nM FAM-labeled negative control #1 siRNA (Ambion, Austin, TX, a siRNA tagged with a derivative of FITC) or nonfluorescent, inactive siControl #3 (Dharmacon, Chicago, IL) for 5 h. Cells were washed twice with PBS, trypsinized, resuspended in PBS with 0.5% FBS, and subjected to 0.4% trypan blue treatment for 30 min to quench the fluorescence of the siRNA adhered on cell surface. Flow cytometry was performed using FACSCalibur (BD Bioscience, USA) with a laser excitation wavelength of 488 nm. Fluorescence detection was obtained using a FL1/FITC detector; 20000 events were recorded for each measurement. Data were analyzed by FlowJo software (version 7.6.4, Tree Star, Inc., Ashland, OR).

To evaluate the effect of carrier on the decline of intracellular siRNA level, the above experiment was repeated in PC3 cells 2 or 7 days after treatment.

Evaluation of siRNA Release and Loss. siRNA release from LPNs and other PEI systems to buffered medium were studied and compared. A 1 mL portion of LPN suspension containing 5 nmol of siRNA was dispersed in 9 mL of RMPI-1640 colorless medium supplemented with 10% v/v phosphate-buffer saline (pH 7.4) at 37 °C. At each time point, a 30 μL aliquot was sampled and transferred to a 96-well microplate, and was incubated with 100 μL of RiboGreen prediluted by 500−2000× with Tris-EDTA buffer (10 mM Tris-HCl, 1 mM EDTA, pH 7.4) at room temperature for 2 min. Fluorescence was measured with SpectroMax microplate reader ($\lambda_{ex}/\lambda_{em}$: 485 nm/530 nm). The amounts of released siRNA were quantified by comparison to a standard curve prepared from siRNA solution at different concentrations mixed with 10 μg blank nanocarriers.

To perform the stability study, 0.5 mL of LPN suspension containing 2.5 nmol negative-siRNA was either lyophilized or dispersed in 4.5 mL medium or 5% dextrose. The samples were incubated at different temperatures (4, 25, 37 °C) for 24 or 100 h. Lyophilized samples were then dispersed with 5 mL RNAase free water. Free, released siRNA molecules in all samples were removed by gel chromatography through a column containing Sephadex G-50 Fine. A 2 mL portion of the suspension was mixed with 2 mL of chloroform to dissolve the lipids to release the retained siRNA. The siRNA in the aqueous layer was quantified by RiboGreen assay as described above. Results were normalized against a fresh LPN sample (assuming retaining 100% siRNA) subjected to the same extraction process.

Fluorescence Imaging of Intracellular siRNA Kinetics. For evaluation of intracellular kinetics, PC3 cells were grown in antibiotic-free colorless RMPI-1460 medium in 35-mm culture dishes each containing a poly-L-lysine coated no. 1 cover glass, and treated with LPNs delivering 80 nM rhodamine-siRNA for 5 h. Transfected cells were reincubated in fresh culture medium at standard cell culture condition. After 2 or 7 days, cells were stained with 2.5 μM DRAQ5 nuclear dye for 5 min and viewed with an Axiostar Plus epifluorescence microscope (Carl Zeiss, Oberkochen, Germany) using Insight camera model 8.0 for image capture. Rhodamine-siRNA and DRAQ5 fluorescences were detected with red channel ($\lambda_{ex}/\lambda_{em}$ = 535 nm/610 nm) and far red channel (shown as pseudoblue, 633 nm/670 nm), respectively. Images were analyzed using Spots Advanced imaging software (v.4.6, Diagnostic Instrument, Sterling Heights, MI).

To rule out the presence of excessive background fluorescence or detection of DRAQ5 in the red channel, the study was repeated using nonfluorescent negative-siRNA. No significant background or DRAQ5-mediated red fluorescence was detected.

Acute Cellular Toxicity Assays. Nonspecific, acute toxicity of carriers on RWPE1 cells and PC3 cells was evaluated using LDH assay (for membrane integrity) and trypan blue exclusion assay (for cell viability). For both assays, cells grown on 24-well plates were treated with PEI, H-PEI, or LPNs loaded with negative-siRNA diluted to a range of concentrations with antibiotic-free medium for 5 h at standard culture conditions. For LDH assay, after treatment the cell growth medium was withdrawn and centrifuged. Supernatant (100 μL/well) was transferred to a 96-well plate. To each well, 100 μL of LDH reaction mixture (LDH cytotoxicity detection kit, Roche, Indianapolis, IN) was added. Absorbance at 500 nm correlating to the leaked LDH level was measured after 0.5 h incubation. For trypan blue assay, cells were lifted after treatment with a cell scraper and stained with 0.1% trypan blue in phosphate-buffered saline. Nonviable, stained cells were counted under a microscope. Data were compared to untreated cells and cells treated with 1 mg/mL PEI which served as the negative and positive controls, respectively.

MTT Assay. PC3 or RWPE1 cells were grown overnight in 96-well plates (seeding density at 5000 cells/well for 2-day group and 2000 cells/well for 5-day group for PC3 cells, 7500 cells/well for 2-day group and 3000 cells/well for 5-day group for RWPE1 cells; the lower PC3 cell density was used because of their faster growth) in antibiotic-free medium. Cells were treated with carriers loaded with negative-siRNA for 48 h, then washed and reincubated in 100 μL of fresh medium. For 2-day group, transfected cells were incubated with 0.5 mg/mL 3-(4,5-dimethylthiazol-2-yl)-2,5-diphenyltetrazolium bromide (MTT) at 37 °C for 2 h followed by 200 μL of DMSO per well for 1 h. Concentrations of the solubilized metabolized dye formed in viable cells were measured by a microplate reader at 570 nm with a reference wavelength at 690 nm. For the 5-day group, transfected cells were incubated at standard culture conditions for 3 additional days, and subjected to the MTT assay as described above.

Clonogenic Assay. The toxicity effect of LPNs against cell proliferation was evaluated with clonogenic assays. RWPE1 or PC3 cells grown in 6-well plates were treated with different carriers loading negative-siRNA for 5 h. Treated cells were reseeded onto 6-cm culture dishes at a density of 100 or 1000 cells per dish, and allowed to proliferate in drug-free culture medium at standard cell culture conditions. The macroscopic colonies (>50 cells in a colony) formed from the proliferating cells after 10 to 14 days were fixed and stained with 0.5% solution of methylene blue in methanol and their numbers counted. The fraction of cells forming cell colonies in each treatment was normalized against the untreated control.

Evaluate Time-Profile of *in vitro* siRNA Activity with Western Immunoblotting. PC3 cells grown to 30−50% confluence in 6-cm culture dishes in antibiotic-free medium were treated with 50 nM

survivin-siRNA delivered using different carriers. After 5 h treatment cells were washed with PBS and reincubated in fresh medium at standard culture conditions. Cells were passaged every 4 days to avoid overgrowth. At predetermined time points up to 11 days after transfection, cells were collected and extracted with Pierce m-PER Mammalian Protein Extraction Reagent supplemented with 0.2%v/v protease inhibitor cocktail P8340 (Sigma-Aldrich, St. Louis, MO). Cell lysates (25 μg of protein per lane) were resolved on a 15% SDS-polyacrylamide gel and electrotransferred onto a 0.45 μm Immobilon-P polyvinylidene difluoride membrane. Membranes were blocked with Tris-buffered saline containing 5% dry skim milk powder and 0.1% Tween 20. Survivin and β-actin were detected with rabbit survivin monoclonal antibody (1:1000) and β-actin antibody AC-40 (1:1500), respectively, followed by horseradish peroxidase conjugated antirabbit IgG (1:4000 for survivin, 1:5000 for β-actin). Proteins were visualized using enhanced chemiluminescence (Pierce, Rockford, IL) and band intensities analyzed using ImageJ software (NIH, Bethesda, MD).

RT-PCR Study. Survivin mRNA expression was quantified as previously described.[53] Total RNA was isolated from cells using Tri Reagent (MRC Inc., Cincinnati, OH). The mRNA expression for survivin and glyceraldehyde-3-phosphate dehydrogenase (GADPH) was determined using a one-step RT PCR kit from Qiagen. The primer used were 5′-GAG GCT GGCTTC ATC CAC TG-3′ (forward) and 5′-CAG CTG CTC GAT GGC ACG GC-3′ (reverse) for survivin, and 5′-GCT TCC CGT TCT CAG CCT TGA C-3′ (forward) and 5′-ATG GGA AGG TGA AGG TCG GAG-3′ (reverse) for GAPDH. Cycling conditions were as follows: initial denaturation at 95 °C for 2 min followed by 30 cycles at 95 °C for 60 s, 62 °C for 30 s, and 72 °C for 7 min. The PCR products were verified by gel electrophoresis.

Evaluate *in Vivo* siRNA Activity. Immunohistochemical staining and image analysis was conducted to evaluate the *in vivo* functionality of siRNA delivered by LPNs. Treatment involved a 100 μL single dose of survivin-siRNA (0.5 nmol) loaded in LPNs suspended in 5% dextrose administered by tail-vein injection 7 days after tumor initiation. Comparison was made against vehicle control (5% dextrose), LPNs delivering inactive siRNA, and H-PEI delivering survivin-siRNA. Animals were sacrificed by CO_2 overexposure 2 or 7 days after treatment and tumors were extracted, blot-dried, fixed in 10% buffered formalin and embedded in paraffin wax. Tumors were sectioned to 5 μm-thickness and the sections were immunostained using goat polyclonal IgG against survivin (C-19) as primary antibody (1:200 dilution) and horseradish peroxidase conjugated antigoat IgG (1:1000 dilution) as secondary antibody, lightly counter-stained with hematoxylin and examined under a microscope (20X objective) connected to a Canon Powershot A640 camera. Tumor survivin levels in the images recorded were analyzed using ImageJ software (NIH, Bethesda, MD) as in our previous study.[35] Briefly, the brownness indicating the survivin level was isolated using the color deconvolution pluggin (using vector: H DAB option). The integrated density of the brownness in each deconvoluted image was normalized against the tumor area (the pixel number occupied by the tumor in the image) determined using the histogram function of Adobe Photoshop (version CS3).

Tumor size was monitored using a caliper every day, and tumor volume was calculated by the standard ellipsoid formula: length $\times$ width^2 $\times$ 0.5236 (π/6). Body weights of animals were also daily monitored.

Statistical Analysis. Differences between groups were assessed using one-way ANOVA and unpaired two-tailed Student's *t*-test, and $p < 0.05$ was considered statistically significant unless otherwise specified.

Acknowledgment. The authors thank Dr. L. Rotkina at Penn Regional Nanotechnology Facility, University of Pennsylvania, and Dr. X. Fan at Flow Cytometry Core Facility, Temple University School of Medicine, for the technical assistance in electron microscopy imaging and flow cytometry, respectively. The study was supported by Pennsylvania Tobacco FY2008 Concept Award.

Supporting Information Available: Results of quantitative siRNA uptake measurement, NMR characterization of H-PEI, and complexation study of siRNA with H-PEI (Figures S1−S3). This material is available free of charge *via* the Internet at http://pubs.acs.org.

REFERENCES AND NOTES

1. Fire, A.; Xu, S.; Montgomery, M.; Kostas, S.; Driver, S.; Mello, C. Potent and Specific Genetic Interference by Double-Stranded RNA in *Caenorhabditis elegans*. *Nature* **1998**, *391*, 806–811.
2. Mello, C. C.; Conte, D., Jr. Revealing the World of RNA Interference. *Nature* **2004**, *431*, 338–342.
3. Heidenreich, O. Targeting Oncogenes with siRNAs. *Methods Mol. Biol.* **2009**, *487*, 221–242.
4. Pirollo, K. F.; Chang, E. H. Targeted Delivery of Small Interfering RNA: Approaching Effective Cancer Therapies. *Cancer Res.* **2008**, *68*, 1247–1250.
5. Kumar, L. D.; Clarke, A. R. Gene Manipulation Through the Use of Small Interfering RNA (siRNA): From *in Vitro* to *in Vivo* Applications. *Adv. Drug Delivery Rev.* **2007**, *59*, 87–100.
6. Reischl, D.; Zimmer, A. Drug Delivery of siRNA Therapeutics: Potentials and Limits of Nanosystems. *Nanomedicine* **2009**, *5*, 8–20.
7. Wang, J.; Lu, Z.; Wientjes, M. G.; Au, J. L.-S. Systemic siRNA Delivery: Barriers and Carriers. *AAPS J.* **2010**, *12*, 492–503.
8. Hongtao, L. V.; Zhang, S.; Wang, B.; Cui, S.; Yan, J. Toxicity of Cationic Lipids and Cationic Polymers in Gene Delivery. *J. Controlled Release* **2006**, *114*, 100–109.
9. Hunter, A. C.; Moghimi, S. M. Cationic Carriers of Genetic Material and Cell Death: A Mitochondrial Tale. *Biochim. Biophys. Acta* **2010**, *1797*, 1203–1209.
10. Hunter, A. C. Molecular Hurdles in Polyfectin Design and Mechanistic Background to Polycation Induced Cytotoxicity. *Adv. Drug Delivery Rev.* **2006**, *58*, 1523–1531.
11. Breunig, M.; Lungwitz, U; Liebl, R.; Goepferich, A. Breaking up the Correlation between Efficacy and Toxicity for Nonviral Gene Delivery. *Proc. Natl. Acad. Sci. U.S.A.* **2007**, *104*, 14454–14459.
12. Godbey, W. T.; Wu, K. K.; Mikos, A. G. Poly(ethylenimine)-Mediated Gene Delivery Affects Endothelial Cell Function and Viability. *Biomaterials* **2001**, *22*, 471–480.
13. Ahn, C. H.; Chae, S. Y.; Bae, Y. H.; Kim, S. W. Biodegradable Poly(ethylenimine) for Plasmid DNA Delivery. *J. Controlled Release* **2002**, *80*, 273–282.
14. Jere, D.; Jiang, H. L.; Arote, R.; Kim, Y. K.; Choi, Y. J.; Cho, M. H.; Akaike, T.; Cho, C. S. Degradable Polyethylenimines as DNA and Small-Interfering RNA Carriers. *Expert Opin. Drug Delivery* **2009**, *6*, 827–834.
15. Demeneix, B; Behr, J. P. Polyethylenimine (PEI). *Adv. Genet.* **2005**, *53*, 217–230.
16. Dehshahri, A; Oskuee, R. K.; Shier, W. T.; Hatefi, A.; Ramezani, M. Gene Transfer Efficiency of High Primary Amine Content, Hydrophobic, Alkyl-Oligoamine Derivatives of Polyethylenimine. *Biomaterials* **2009**, *30*, 4187–4194.
17. Shim, M. S.; Kwon, Y. J. Acid-Responsive Linear Polyethylenimine for Efficient, Specific, and Biocompatible siRNA Delivery. *Bioconjugate Chem.* **2009**, *20*, 488–499.
18. Bonnet, M. E.; Erbacher, P.; Bolcato-Bellemin, A. L. Systemic Delivery of DNA or siRNA Mediated by Linear Polyethylenimine (L-PEI) does not Induce an Inflammatory Response. *Pharm. Res.* **2008**, *25*, 2972–2982.
19. Fukumoto, Y.; Obata, Y.; Ishibashi, K.; Tamura, N.; Kikuchi, I.; Aoyama, K.; Hattori, Y.; Tsuda, K.; Nakayama, Y.; Yamaguchi, N. Cost-Effective Gene Transfection by DNA Compaction at pH 4.0 Using Acidified, Long Shelf-Life Polyethylenimine. *Cytotechnology* **2010**, *62*, 73–82.
20. Masotti, A.; Moretti, F.; Mancini, F.; Russo, G.; Di Lauro, N.; Checchia, P.; Marianecci, C.; Carafa, M.; Santucci, E.; Ortaggi, G. Physicochemical and Biological Study of Selected Hydrophobic Polyethylenimine-Based Polycationic Liposomes and Their Complexes with DNA. *Bioorgan. Med. Chem.* **2007**, *15*, 1504–1515.
21. Yamazaki, Y.; Nango, M.; Matsuura, M.; Hasegawa, Y.; Hasegawa, M.; Oku, N. Polycation Liposomes, A Novel Nonviral Gene Transfer System, Constructed from Cetylated Polyethylenimine. *Gene Ther.* **2000**, *7*, 1148–1155.

22. Raemdonck, K.; Vandenbroucke, R. E.; Demeester, J.; Sanders, N. N.; De Smedt, S. C. Maintaining the Silence: Reflections on Long-Term RNAi. *Drug Discovery Today* **2008**, *13*, 917–931.
23. Wong, H. L.; Rauth, A. M.; Bendayan, R.; Wu, X. Y. Combinational Treatment with Doxorubicin and GG918 (Elacridar) Using Polymer-Lipid Hybrid Nanoparticles (PLN) and Evaluation of Strategies for Multidrug-Resistance Reversal in Human Breast Cancer Cells. *J. Controlled Release* **2006**, *116*, 275–284.
24. Wong, H. L.; Bendayan, R.; Rauth, A. M.; Xue, H. Y.; Babakhanian, K.; Wu, X. Y. A Mechanistic Study of Enhanced Doxorubicin Uptake and Retention in Multidrug Resistant Breast Cancer Cells Using a Polymer-Lipid Hybrid Nanoparticle (PLN) System. *J. Pharmacol. Exp. Ther.* **2006**, *317*, 1372–1381.
25. Muller, R. H.; Karsten, M.; Sven, G. Solid Lipid Nanoparticles (SLN) for Controlled Drug Delivery—A Review of the State of the Art. *Eur. J. Pharm. Biopharm.* **2000**, *50*, 161–177.
26. Wong, H. L.; Bendayan, R.; Rauth, A. M.; Wu, X. Y. Development of Solid Lipid Nanoparticles Containing Ionically Complexed Chemotherapeutic Drugs and Chemosensitizers. *J. Pharm. Sci.* **2004**, *93*, 1993–2008.
27. Wong, H. L.; Bendayan, R.; Rauth, A. M.; Li, Y.; Wu, X. Y. Chemotherapy with Anticancer Drugs Entrapped into Solid Lipid Nanoparticles. *Adv. Drug. Delivery Rev.* **2007**, *59*, 491–504.
28. Van de Ven, H.; Vermeersch, M.; Shunmugaperumal, T.; Vandervoort, J.; Maes, L.; Ludwig, A. Solid Lipid Nanoparticle (SLN) Formulations as a Potential Tool for the Reduction of Cytotoxicity of Saponins. *Pharmazie* **2009**, *64*, 172–176.
29. Xue, H. Y.; Wong, H. L. Tailoring Nanostructured Solid-Lipid Carriers for Time-Controlled Intracellular siRNA Kinetics to Sustain RNAi-Mediated Chemosensitization. *Biomaterials* **2011**, *32*, 2662–2672.
30. Xu, Z.; Chen, L.; Gu, W.; Gao, Y.; Lin, L.; Zhang, Z.; Xi, Y.; Li, Y. The Performance of Docetaxel-Loaded Solid Lipid Nanoparticles Targeted to Hepatocellular Carcinoma. *Biomaterials* **2009**, *30*, 226–232.
31. del Pozo-Rodriguez, A.; Pujals, S.; Delgado, D.; Solinis, M. A.; Gascon, A. R.; Giralt, E.; Pedraz, J. L. A Proline-Rich Peptide Improves Cell Transfection of Solid Lipid Nanoparticle-Based Nonviral Vectors. *J. Controlled Release* **2009**, *133*, 52–59.
32. Wang, M. T.; Jin, Y.; Yang, Y. X.; Zhao, C. Y.; Yang, H. Y.; Xu, X. F. *In Vivo* Biodistribution, Anti-Inflammatory, and Hepatoprotective Effects of Liver Targeting Dexamethasone Acetate Loaded Nanostructured Lipid Carrier System. *Int. J. Nanomed.* **2010**, *5*, 487–497.
33. Stevens, P. J.; Sekido, M.; Lee, R. J. A Folate-Receptor-Targeted Lipid Nanoparticle Formulation for a Lipophilic Paclitaxel Prodrug. *Pharm. Res.* **2004**, *21*, 2153–2157.
34. Wong, H. L.; Rauth, A. M.; Bendayan, R.; Wu, X. Y. Evaluation of the *in Vivo* Efficacy, Toxicity, and Lymphatic Drainage of Loco-regional Administered Polymer-Lipid Hybrid Nanoparticles (PLN) Loaded with Doxorubicin in a Murine Solid Tumor Model. *Eur. J. Pharm. Biopharm.* **2007**, *65*, 300–308.
35. Aliabadi, H. M.; Landry, B.; Bahadur, R. K.; Neamnark, A.; Suwantong, O.; Uludağ, H. Impact of Lipid Substitution on Assembly and Delivery of siRNA by Cationic Polymers. *Macromol. Biosci.* **2011**, *11*, 662–672.
36. Schäfer, J.; Höbel, S.; Bakowsky, U.; Aigner, A. Liposome—Polyethylenimine Complexes for Enhanced DNA and siRNA Delivery. *Biomaterials* **2010**, *26*, 6892–6900.
37. Wong., H. L.; Shen, Z.; Lu, Z.; Wientjes, M. G.; Au, J. L-S. Paclitaxel Tumor-Priming Enhances siRNA Delivery and Transfection in 3-Dimensional Tumor Cultures. *Mol. Pharmaceut.* **2011**, *8*, 833–840.
38. Pirollo, K. F.; Chang, E. H. Targeted Delivery of Small Interfering RNA: Approaching Effective Cancer Therapies. *Cancer Res.* **2008**, *68*, 1247–1250.
39. Ghonaim, H. M.; Li, S.; Blagbrough, I. S. N1, N12-Diacyl Spermines: SAR Studies on Nonviral Lipopolyamine Vectors for Plasmid DNA and siRNA Formulation. *Pharm. Res.* **2010**, *27*, 17–29.
40. Zelphati, O.; Uyechi, L. S.; Barron, L. G.; Szoka, F. C. Effect of Serum Components on the Physico-Chemical Properties of Cationic Lipid/Oligonucleotide Complexes and on Their Interactions with Cells. *Biochim. Biophys. Acta; Lipids Lipid Metab.* **1998**, *1390*, 119–133.
41. Buyens, K.; Lucas, B.; Raemdonck, K.; Braeckmans, K.; Vercammen, Jo; Hendrix, J.; Engelborghs, Y.; De Smedt, S. C.; Sanders, N. N. A Fast and Sensitive Method for Measuring the Integrity of siRNA-Carrier Complexes in Full Human Serum. *J. Controlled Release* **2008**, *126*, 67–76.
42. Xiong, M. P.; Forrest, M. L.; Ton, G.; Zhao, A.; Davies, N. M.; Kwon, G. S. Poly(aspartate-G-PEI800), a Polyethylenimine Analogue of Low Toxicity and High Transfection Efficiency for Gene Delivery. *Biomaterials* **2007**, *28*, 4889–4900.
43. Zhang, M.; Latham, D. E.; Delaney, M. A.; Chakravarti, A. Survivin Mediates Resistance to Antiandrogen Therapy in Prostate Cancer. *Oncogene* **2005**, *24*, 2474–2482.
44. Rahman, K. M. W.; Banerjee, S.; Ali, S.; Ahmad, A.; Wang, Z.; Kong, D.; Sakr, W. A. 3,3′-Diindolylmethane Enhances Taxotere-Induced Apoptosis in Hormone-Refractory Prostate Cancer Cells Through Survivin Down-Regulation. *Cancer Res.* **2009**, *69*, 4468–4475.
45. Brunsvig, Fr. P.; Andersen, A.; Aamdal, S.; Kristensen, V.; Olsen, H. Pharmacokinetic Analysis of Two Different Docetaxel Dose Levels in Patients with Non-Small Cell Lung Cancer Treated with Docetaxel as Monotherapy or with Concurrent Radiotherapy. *BMC Cancer* **2007**, *7*, 197.
46. Kostka, L.; Konák, C.; Subr, V.; Spírková, M.; Addadi, Y.; Neeman, M.; Lammers, T.; Ulbrich, K. Removable Nanocoatings for siRNA Polyplexes. *Bioconjugate Chem.* **2011**, *16*, 169–179.
47. Mao, S.; Neu, M.; Germershaus, O.; Merkel, O.; Sitterberg, J.; Bakowsky, U.; Kissel, T. Influence of Polyethylene Glycol Chain Length on the Physicochemical and Biological Properties of Poly(ethylene imine)-Graft-Poly(ethylene glycol) Block Copolymer/siRNA Polyplexes. *J. Controlled Release* **2008**, *126*, 67–76.
48. Ambrosini, G.; Adida, C.; Altieri, D. C. A Novel Anti-apoptosis Gene; Survivin; Expressed in Cancer and Lymphoma. *Nat. Med.* **1997**, *3*, 917–921.
49. Singh, R.; Singh, S.; Sharma, P. K.; Lillard, J. W., Jr. T Regulatory and Prostate Cancer Cell-Specific Drug Targeting Using Novel XPclad Nanoparticles. *J. Immunol.* **2009**, *182*, 42.7.
50. Raj, D.; Liu, T.; Samadashwily, G.; Li, F.; Grossman, D. Survivin Repression by p53, Rb and E_2F_2 in Normal Human Melanocytes. *Carcinogenesis* **2008**, *29*, 194–201.
51. Pennati, M.; Folini, M.; Zaffaroni, N. Targeting Survivin in Cancer Therapy: Fulfilled Promises and Open Questions. *Carcinogenesis* **2007**, *28*, 1133–1139.
52. Reibetanz., U.; Halozan, D.; Brumen, M.; Donath, E. Flow Cytometry of HEK 293T Cells Interacting with Polyelectrolyte Multilayer Capsules Containing Fluorescein-Labeled Poly(acrylic acid) as a pH Sensor. *Biomacromolecules* **2007**, *8*, 1927–1933.
53. Ghadersohi, A.; Pan, D.; Fayazi, Z.; Hicks, D. G.; Winston, J. S.; Li, F. Prostate-derived ETS Transcription Factor (PDEF) Downregulates Survivin Expression and Inhibits Breast Cancer Cell Growth *In Vitro* and Xenograft Tumor Formation *In Vivo*. *Breast Cancer Res. Treat.* **2007**, *102*, 19–30.